Supporting Information

Unidirectional Growth of Single-Walled Carbon Nanotubes

Naoki Ishigami, Hiroki Ago,* Tetsushi Nishi, Ken-ichi Ikeda, Masaharu Tsuji, Tatsuya Ikuta, and Koji Takahashi

Graduate School of Engineering Sciences, Institute for Materials Chemistry and Engineering, Kyushu University, Kasuga, Fukuoka 816-8580, Japan PRESTO, Japan Science and Technology Agency (JST), Kawaguchi, Saitama 332-0012, Japan, and Graduate School of Engineering, Kyushu University, Motooka, Fukuoka 819-0395, Japan

E-mail: ago@cm.kyushu-u.ac.jp

Experimental details

1. Pattern definition by photolithography

a-Plane $(1\,1\,\bar{2}\,0)$ and r-plane $(1\,\bar{1}\,0\,2)$ sapphire and ST-cut quartz with an inclined (miscut) angle of less than 0.3° were purchased from KYOCERA Co., Japan and NIHON DEMPA KOGYO Co., LTD., Japan, respectively. The substrates were cleaned by sonicating in acetone and isopropyl alcohol, and then spin-coated the photoresist, TSMR-CR (TOKYO OHKA KOGYO Co., LTD., Japan) for the metal salt patterning or AZ5214-E (AZ ELECTRO MATERIALS K.K., Japan) for the metal film patterning. The stripe openings were created after UV exposure and development. The width of openings was 10 μm, and the distances between the lines were 50 and 100 μm for metal salt and 300 μm for metal films. Electron-beam (EB) lithography also was used to make the narrow pattern with the opening width of 200 nm. For the EB lithography, the r-plane sapphire substrate was spin-coated with an anti-static polymer and ZEP-520A (ZEON Co.), followed by EB exposure and development.

2. Co-Mo salt deposition by dip-coating

The substrate with patterned photoresist was introduced into the aqueous solution of cobalt (II) nitrate hexahydrate ($Co(NO_3)_2 \cdot 6H_2O$) and bis(acetylacetonate)dioxomolybdenum ($MoO_2(acac)_2$) with an atomic ratio of Co:Mo = 94:6 and then pulled up from the solution at a rate of 5 mm/min. After drying the substrates on a hot plate at 100 °C, the excess photoresist and catalyst were lift-off in acetone.

3. Fe and Co film deposition by a magnetron sputtering

The mask with a slit was used for producing Fe and Co films with a gradual change in the thickness (Fig. S1). The substrate with patterned photoresist was placed 4.9 mm below the mask with a 2mm-width slit. The distance from the center of the slit to the origin of the pattern was set 4.0 mm. A film of Fe or Co was deposited on the substrate through the slit by a magnetron sputtering (Shibaura Mechatronics Co., CFS-4ES) in Ar atmosphere at 0.6 Pa, and then the photoresist was lift-off in acetone.

4. Nanotube growth

SWNTs were synthesized by chemical vapor deposition (CVD) in a 26 mm diameter quartz tube, using 900/100 or 300/80 sccm flow of CH_4/H_2 under atmospheric pressure at 900 °C. Prior to the introduction of the CH_4 gas, the catalyst was reduced with H_2 gas for 5-10 min at the same temperature.

5. Characterization

The structures of the as-grown SWNTs and catalysts were studied with an atomic force microscopy (AFM, Veeco Nanoscope IIIa) and a scanning electron microscopy (SEM, HITACHI S-4800).

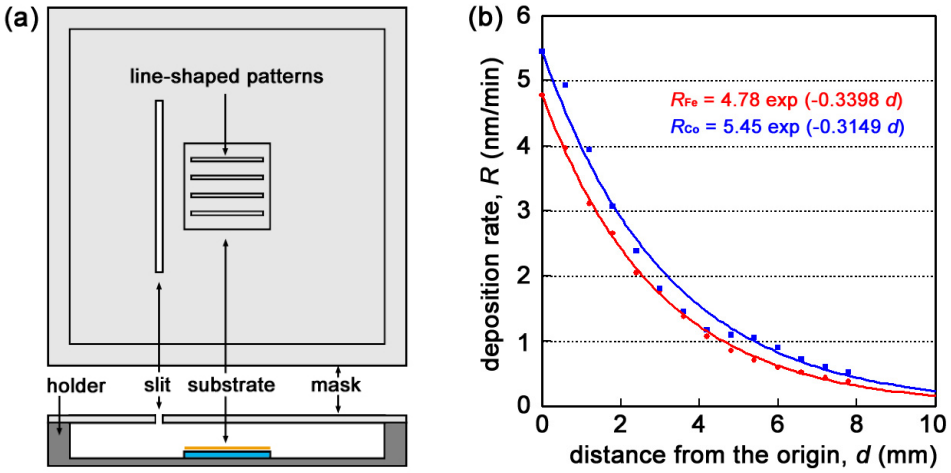

Figure S1. (a) Schematic view of the preparation of the gradual thin film reported by Noda et al.[14] (b) Deposition rate profiles of Fe and Co films. Their thicknesses decrease exponentially with the distance from the origin.

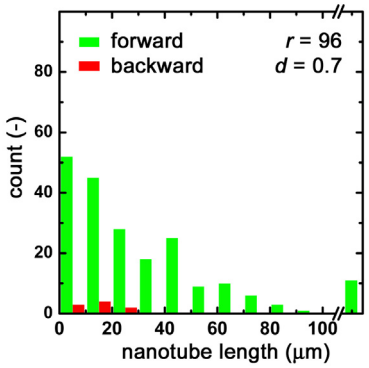

Figure S2. Histogram of the length distribution of SWNTs grown from the Co-Mo salt catalyst on r-plane sapphire substrate. The corresponding SEM image is shown in Fig. 1. The SWNTs grown from a catalyst line with a length of 300 μm was counted. The r and d are the ratio of the forward SWNTs ($r = N_{forward}/(N_{forward} + N_{backward})\times100$) (%) and tube density ($d = (N_{forward} + N_{backward})/300$ μm) (μm^{-1}), respectively.

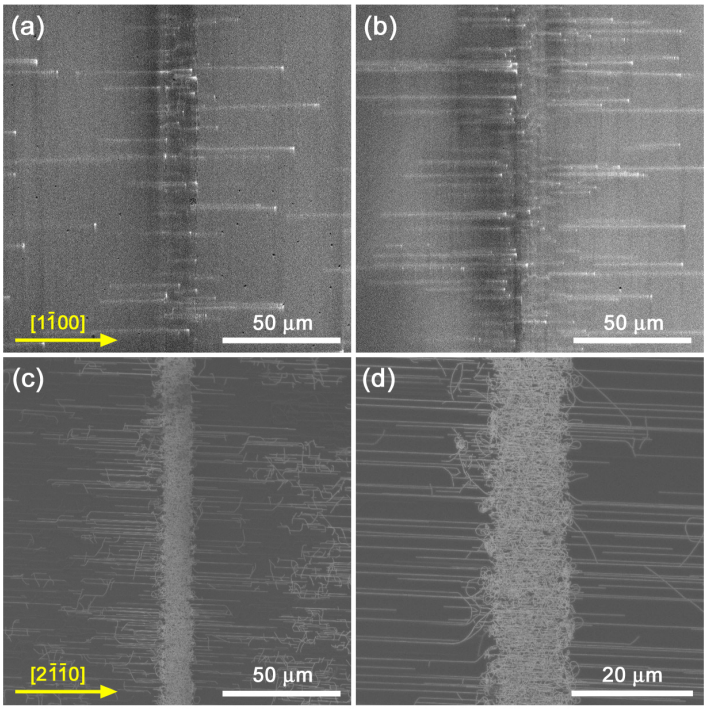

Figure S3. SEM images of aligned SWNTs grown on (a), (b) a-plane sapphire and (c), (d) ST-cut quartz substrates. The SWNTs were grown with (a), (c), (d) Co-Mo salt and (b) Fe film (1 nm) catalysts. The aligned SWNTs grow along the $[1\ \bar{1}\ 0\ 0]$direction on a-plane sapphire and the $[2\ \bar{1}\ \bar{1}\ 0]$ direction on ST-cut quartz, respectively. The right end of a SWNT on the *a*-plane appears bright, because the SEM image was captured by scanning from the right to left, and this phenomenon often occurs in low-density SWNTs.

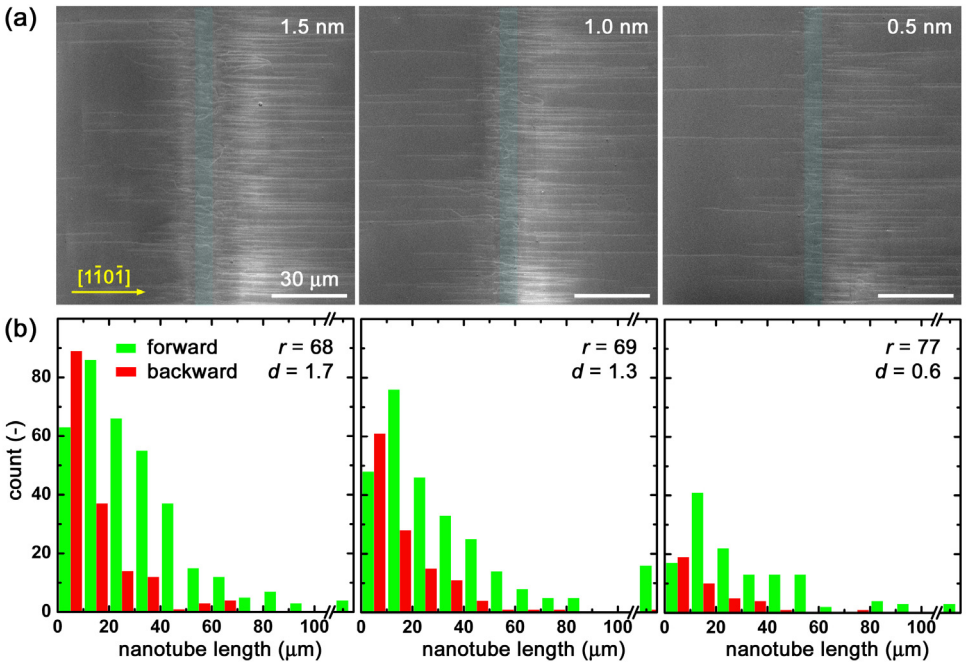

Figure S4. (a) SEM images of the aligned SWNTs grown from the patterned Co thin film catalyst with different film thicknesses on r-plane sapphire substrate. (b) Histograms of the length distribution of SWNTs. The SWNTs grown from a catalyst line with the length of 300 μm were counted.

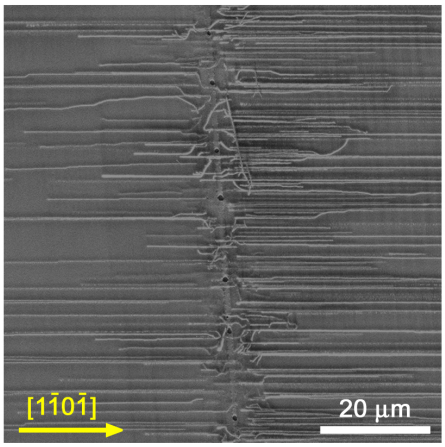

Figure S5. SEM image of aligned SWNTs from the Fe film line with a thickness of 1.0 nm defined by EB lithography on r-plane sapphire substrate. The some of SWNTs grow to the backward direction even though the line width is very narrow (200 nm). This result signifies that the backward growth is not attributed to the excessive amount of catalyst.

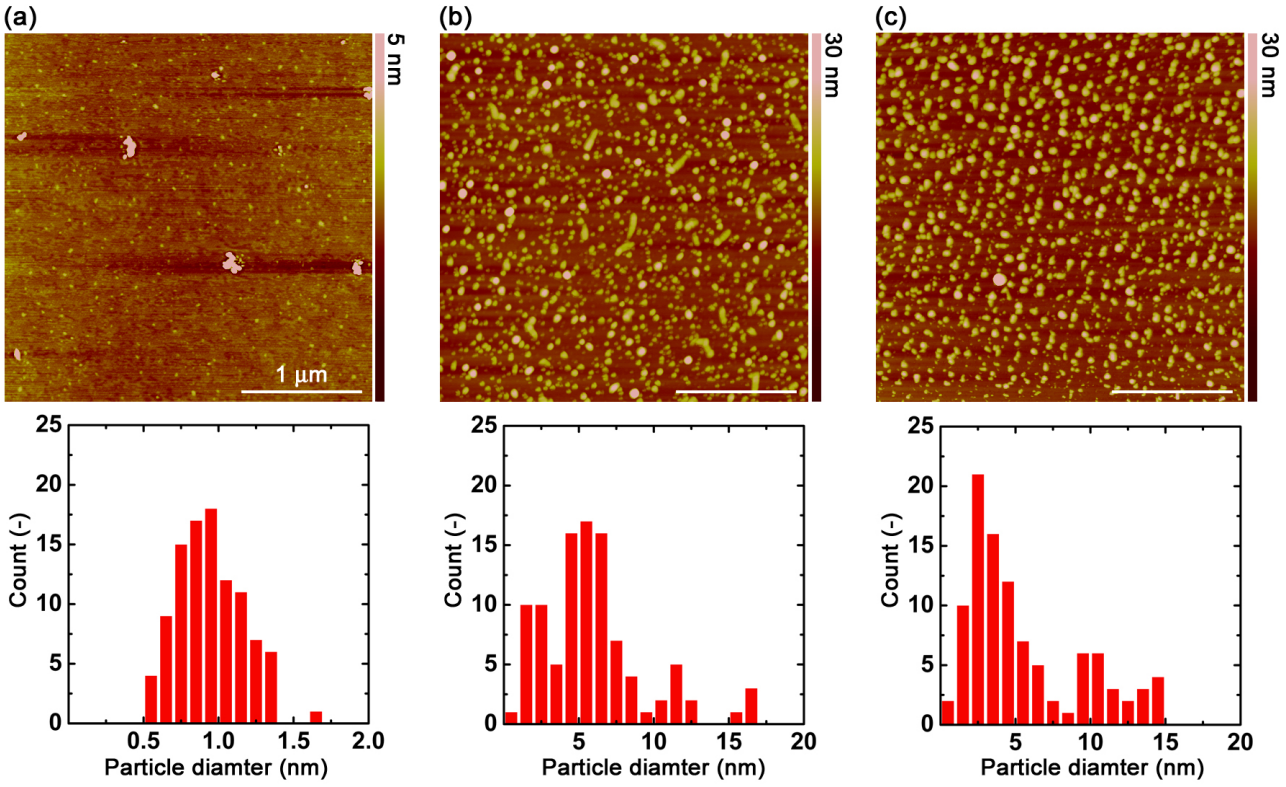

Figure S6. AFM images and diameter distributions of metal nanoparticles derived from (a) Co-Mo salt, (b) 0.5 nm Fe film, and (c) 0.5 nm Co film on r-plane sapphire substrates. It is seen that the Co-Mo salts gave much smaller metal nanoparticles with a narrower distribution compared with the sputtered Fe/Co films. These images were obtained after heat treatment in H_2 at 900 ^{o}C for 10 min. The total number of counted metal nanoparticles is 100.

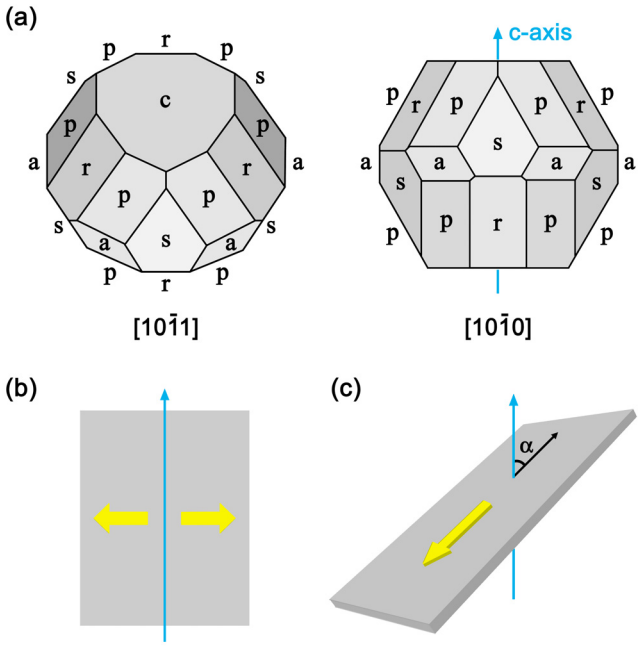

Figure S7. (a) Equilibrium shape of a sapphire crystal viewed from the $[1\ 0\ \bar{1}\ 1]$ and $[1\ 0\ \bar{1}\ 0]$ directions.[S1] The shape consists of a- $(1\ 1\ \bar{2}\ 0)$, r- $(1\ \bar{1}\ 0\ 2)$, c- $(0\ 0\ 0\ 1)$, s- $(1\ 0\ \bar{1}\ 1)$ and p- $(1\ 1\ \bar{2}\ 3)$ planes. The crystallographic axis referred to c-axis is perpendicular to c-plane. Schematic diagrams of the surface on (b) a-plane and (c) r-plane, where the blue and yellow arrow indicates c-axis and growth direction of SWNTs. The angle α between c-axis and r-plane surface is 32.4°.

Reference

(S1) Hockey, B. J.; Wiedrhorn, S. M.; Handwerker, C. A.; Blendell, J. E.; Carter, W. C.; Roosen, A. R. *J. Am. Ceram. Soc.* **1997**, *80*, 62.